Hindawi Publishing Corporation
Journal of Nanomaterials
Volume 2016, Article ID 9174085, 8 pages
http://dx.doi.org/10.1155/2016/9174085

Research Article

Thermal Transport Properties of Dry Spun Carbon Nanotube Sheets

Heath E. Misak, James L. Rutledge, Eric D. Swenson, and Shankar Mall

Department of Aeronautics and Astronautics, Air Force Institute of Technology, 2950 Hobson Way, Wright-Patterson AFB, OH 45433-7765, USA

Correspondence should be addressed to Shankar Mall; Shankar.Mall@afit.edu

Received 14 December 2015; Revised 1 February 2016; Accepted 16 February 2016

Academic Editor: Yasuhiko Hayashi

The thermal properties of carbon nanotube- (CNT-) sheet were explored and compared to copper in this study. The CNT-sheet was made from dry spinning CNTs into a nonwoven sheet. This nonwoven CNT-sheet has anisotropic properties in in-plane and out-of-plane directions. The in-plane direction has much higher thermal conductivity than the out-of-plane direction. The in-plane thermal conductivity was found by thermal flash analysis, and the out-of-plane thermal conductivity was found by a hot disk method. The thermal irradiative properties were examined and compared to thermal transport theory. The CNT-sheet was heated in the vacuum and the temperature was measured with an IR Camera. The heat flux of CNT-sheet was compared to that of copper, and it was found that the CNT-sheet has significantly higher specific heat transfer properties compared to those of copper. CNT-sheet is a potential candidate to replace copper in thermal transport applications where weight is a primary concern such as in the automobile, aircraft, and space industries.

1. Introduction

Carbon nanotubes have received immense attention from researchers due to their extraordinary mechanical and physical properties [1–3]. Utilizing this nanosized material on the bulk level while retaining these extraordinary properties has been found to be difficult. One such promising method is to use a spinning process to entangle individual CNTs into infinite long bulk sheets and yarns [4]. While there is limited work done with the microstructure of sheets, considerable work has been done with the CNT-yarns. It has been found that CNT-yarns contain substructures within the yarn: (1) individual CNTs, (2) bundled CNTs, (3) ribbons composed of bundled CNTs, and (4) finally yarns made from twisted ribbons [5]. These structures can reduce the strength due to stress concentrators, and it has been found that CNT-yarns are sensitive to kink-band failure, tearing, and wear [6]. During the straining process, the CNT-yarns move across each other forming the defects. This has produced mechanical properties lower than expected in multiyarns, while small diameter single yarns have shown some impressive results [7–11]. Further, when considering electrical properties, the end-to-end gap of the individual CNTs has been found to be critical in electron transport leading to improved properties by compression, and consolidation of CNT-yarns [12–16].

There has been limited reporting on the thermal transport properties of CNT-yarns and sheets; however, considerable research has been done on the thermal transport properties of individual CNTs. Marconnet et al. have performed a review of literature detailing previous work [17]. They found that CNTs had thermal conductivity ranging from 13,350 to 34 W/mK [18, 19]. There are many reasons for this large range of thermal conductivity including (1) number of CNT walls, (2) CNT diameter, (3) length (how it was measured), (4) boundary conditions, (5) CNT-defects, and (6) chiralities. Choi et al. used the 2-pad 3ω technique to measure the thermal conductivity and found a 42 nm carbon nanotube with a length of 1.1 μm to have a thermal conductivity of 830 W/mK [20]. This is a very high thermal conductivity considering the conductivity of copper is ~380 W/mK at room temperature [21].

The thermal conductivity of an individual CNT is exceptional and has led to much attention towards producing a higher thermally conductive composite composed of a polymer base matrix and carbon nanotubes [22–24]. It has been found that, by adding 1% of CNTs to epoxy, the thermal conductivity can be raised by 125% at room temperature [22]. While this is an impressive increase, the thermal conductivity of the CNT-epoxy composite (~0.5 W/mK) is much lower than copper. A 10% by weight of CNT in polystyrene composite produced thermal conductivity of ~0.35 W/mK [23]. In this case, the objective was not to increase the thermal conductivity, but to alter other properties, that is, foams with large expansion ratio (18-fold) and a macrocellular cell size (5 μm). While adding CNTs to the matrix increases the thermal conductivity over the polymer matrix, its thermal conductivity is not comparable to copper.

Some limited research has been done on the thermal conductivity of pure CNT materials [25–28]. These yarns are 10 μm in diameter and were found to have a room temperature thermal conductivity of 60 ± 20 W/mK [25]. In the same study, it was found that with increase of diameter the properties decreased, and it was attributed to structural differences. A larger diameter yarn (34 μm) was found to have a thermal conductivity of 25 ± 6 W/mK compared to the smaller diameter (10 μm) with a thermal conductivity of 60 ± 20 W/mK. Research has been done on high-density carbon nanotube buckypaper which showed excellent thermal transport properties. The density was reported to be extremely high at 1.39 g/cm^3, which is the density of an individual CNT, and resulted in a thermal conductivity of 766 W/mK [26]. Others have not seen such high thermal conductivities or densities. Li and Yue found that CNT buckypaper has a conductivity of 0.83 W/mK [27]. Aliev et al. found that the thermal conductivity of CNT-sheet to be 50 ± 5 W/mK. They show the low thermal conductivity of the CNT-sheet when compared to individual CNTs is due to tube-tube interconnections and sheet imperfections [28].

In the present study, a CNT-sheet was investigated for the thermal properties and its applications towards thermal management with an eventual goal of replacing the copper sheet. Laser flash analysis was used to determine the in-plane thermal diffusivity. The density and specific heat were measured to determine the in-plane thermal conductivity. The out-of-plane thermal conductivity was measured by hot disk technique. The thermal emittance properties were probed by an IR camera under a vacuum environment, and the resultant empirical data were compared to thermal transport theory. Finally, the CNT-sheet's thermal properties are compared with those of a comparable copper sheet painted with flat black on one side.

2. Methods and Materials

2.1. Material. The CNT-sheet was procured from Nanocomp Inc. A dry spinning process was used to form the CNT-sheets. This was done by feeding carbon based gases into a reactor with catalyst at high temperatures. The carbon is absorbed into the catalyst and thereby CNTs are formed. The CNTs are in a form similar to an "aerogel" or what is called a smock.

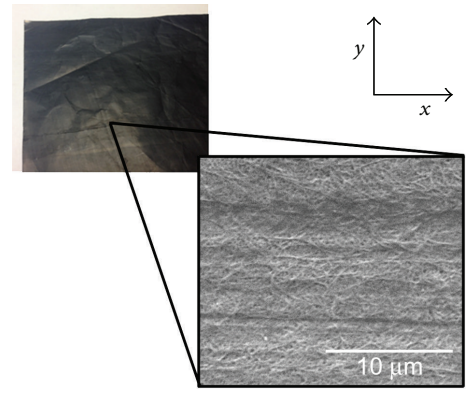

Figure 1: Bulk CNT-sheet showing magnified region containing multitudes of CNTs.

The smock is then collected and formed into a CNT-sheet. Consolidation was done by acetone dip without any further treatments. Figure 1 shows the bulk CNT-sheet obtained by an optical camera, and the magnified region was imaged with a scanning electron microscope (SEM) showing multitudes of CNTs. This CNT-sheet is considered a nonwoven material with an areal density of 10–15 g/m^2. Others have reported similar manufacturing processes [4, 29].

2.2. Thermal Transport

2.2.1. Laser Flash Analysis. CNT-sheet is thin and highly thermally conductive for conventional thermal analysis methods; however, laser flash analysis can be used to find the thermal diffusivity (α) as done in this work. The thermal conductivity (k) can be determined after the thermal diffusivity is measured by combining with the density (ρ) and specific heat (c) from (1). In this work, Nietzsche LFA 457 and Proteus LFA analysis software was used to find α. Specimens were cut to 25.4 mm diameter before running tests:

$$k = \alpha \rho c. \tag{1}$$

2.2.2. Density and Specific Heat. The density was calculated by simply dividing the weight by the volume. An Ohaus Voyager Pro microbalance was used to weigh the specimen. Specimens were cut to the dimensions of 25.4 × 25.4 mm. The area of the specimen was measured by calipers with visible contact on both sides of the calipers, and the thickness was measured using a Rex MTG-DX Durometer with an 8 g weight and 16 mm diameter pressor foot for each specimen. The specific heat was found using a Q100 TA Instrument DSC.

2.3. Thermal Conductivity. For the out-of-plane thermal conductivity, a Hot Disk TPS 2500S utilizing a thin film sensor was used. The hot disk method is optimized for low thermal conductivities and thin samples, making it a better choice for out-of-plane thermal conductivity measurements than the laser flash analysis [30]. The laser flash analysis works well for in-plane measurements; thus, the in-plane thermal conductivity was found by using (1) [31, 32]. Three specimens measuring 25.4 × 25.4 mm were tested in each case.

2.4. Thermal Emittance. The heat flux in the y direction (q_y) within an object is given by

$$q_y = -k\frac{\partial T}{\partial y}. \tag{2}$$

In this presented research, one end of a rectangular sheet of material was heated uniformly under a vacuum (10^{-5} Torr) such that heat transfer would be one-dimensional in the y direction, and the y direction is the distance from the heater. The temperature was measured with infrared thermography. The vacuum eliminated convection as a heat loss mechanism. Therefore, only thermal emittance would be responsible for a variation in q_y in the y direction, giving rise to a nonzero value of $\partial^2 T/\partial y^2$. It can be readily seen that the conduction heat transfer is balanced with thermal emittance through (the right side of the equation is 0 at steady state)

$$\alpha\frac{\partial^2 T}{\partial y^2} + \frac{(\varepsilon_1 + \varepsilon_2)\,\sigma\left(T_{\text{surr}}^4 - T^4\right)}{\rho c L} = 0 \tag{3}$$

or

$$C_{\text{Equation (3)}} + R_{\text{Equation (3)}} = 0, \tag{4}$$

where

$$C_{\text{Equation (3)}} = \alpha\frac{\partial^2 T}{\partial y^2},$$
$$R_{\text{Equation (3)}} = \frac{(\varepsilon_1 + \varepsilon_2)\,\sigma\left(T_{\text{surr}}^4 - T^4\right)}{\rho c L}. \tag{5}$$

In (3), ε_1 and ε_2 are the emissivities at 10 μm wavelength on each side of the sheet, σ is the Stefan-Boltzmann constant, T is temperature, T_{surr} is the ambient temperature, ρ is the density, c is the specific heat, L is the sheet thickness, and y is the position along the length of the sheet. In the case of the copper sample, one side was painted black to improve the IR readings, and this increased emissivity was taken into account through the two emissivities noted in (3). Equations (4) and (5) represent (3) broken down into distinct components that will be used to describe thermal transport theory as it relates to the empirical data. Equation (6) shows the normalized error calculation between $C_{\text{Equation (3)}}$ and $R_{\text{Equation (3)}}$:

$$\text{Normalized Error} = \frac{\left(C_{\text{Equation (3)}} - R_{\text{Equation (3)}}\right)}{C^{\circ}_{\text{Equation (3)}}}, \tag{6}$$

where $C^{\circ}_{\text{Equation (3)}}$ is the $C_{\text{Equation (3)}}$ value at a distance of 0 mm from the heater.

The tests were conducted in a vacuum chamber with a heater powered by a 6033A Agilent power source. The power source was controlled by an in-house designed Labview program. The IR camera was FLIR SC640, and the windows the camera looked through were made of zinc selenide. IR spectra range of the camera is 7.5 to 13 μm. Calibration of the IR counts to temperature was done from a K-type thermal couple on the back of specimens. The temperature range of interest was between 313 and 373 K.

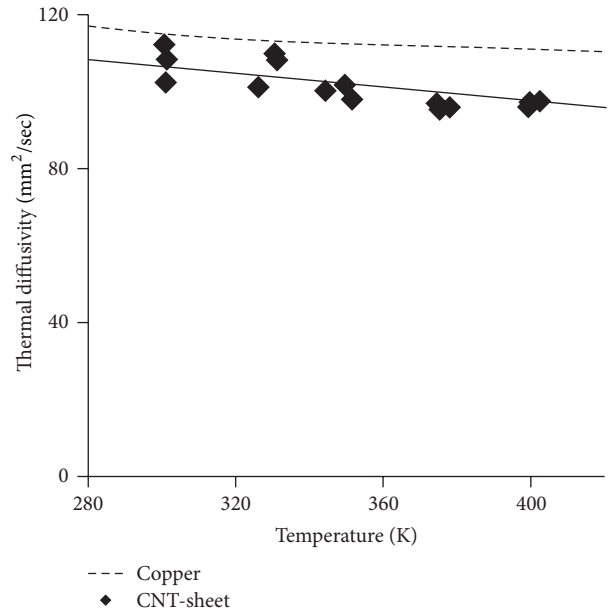

Figure 2: Thermal diffusivity of CNT-sheet and copper versus temperature showing a slightly reduced thermal diffusivity for CNT-sheet compared to copper.

3. Results and Discussion

3.1. CNT-Sheet. The CNT-sheet tested is composed of multitudes of aligned CNTs that are held together by multitude of forces that are still under debate but includes van der Waals bonds and mechanical interlocking [33–35]. The CNTs are aligned in two directions, and the individual CNT diameter is ~50 nm. This directionality results in anisotropic properties, and it is expected that out-of-plane and in-plane properties are considerably different. The thickness of the CNT-sheet was found to be 40 ± 1.7 nm, and the density was found to be 0.39 ± 0.006 g/cm^3.

3.2. Thermal Diffusivity. As described by (1), it is necessary to find α to determine the in-plane thermal conductivity of the CNT-sheet. This can be done with thermal flash analysis, and the data can be seen in Figure 2 (as diamond). Also for the comparison, copper (dashed line) which is considered the "gold standard" for applications requiring high thermal conductivity is included. From this data, it is clearly seen that the CNT-sheet's α is close to that of copper within ~87% to 96%. This shows that heat moves through CNT-sheet at approximately at the same rate as in the copper. For both the copper and the CNT-sheet, there is a slight drop in α with the increasing temperature.

3.3. Volumetric Heat Capacity. The volumetric heat capacity is the density (ρ) multiplied by the specific heat (c). This is significant as it describes the ability of a given volume of substance to store internal energy while undergoing a given temperature change, but without a phase transformation. For a fast thermal cycling system, it is ideal to have a low volumetric heat capacity; however, a high volumetric

Table 1: Thermal properties of CNT-sheet and copper at room temperature.

	Thermal diffusivity (mm^2/sec)	Specific heat (W/gK)	Density (g/cm^3)	In-plane thermal conductivity (W/mK)	In-plane specific thermal conductivity ($W/mK/g/cm^3$)	Out-of-plane thermal conductivity (W/mK)
CNT-sheet	108 ± 5	0.62 ± 0.01	0.39 ± 0.006	25 ± 1.2	64 ± 3	0.1 ± 0.01
Copper	115	0.39	8.9	380	43	380

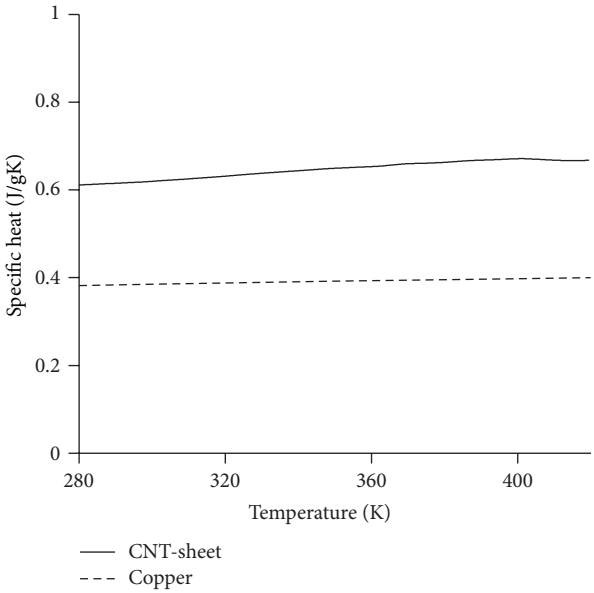

Figure 3: Specific heat of CNT-sheet and copper versus temperature showing CNT-sheet performs better than copper.

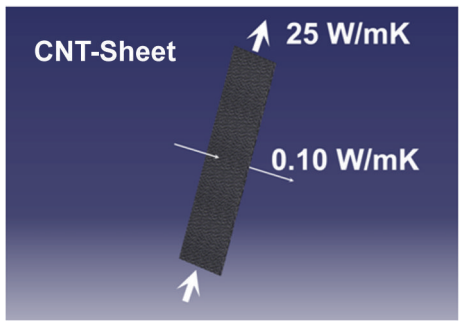

Figure 4: In-plane and out-of-plane thermal conductivities of CNT-sheet.

heat capacity also increases the thermal conductivity. When comparing CNT-sheet to copper, there is a distinct difference. Copper has significant larger density (8.9 g/cm^3) compared to CNT-sheet (0.39 ± 0.006 g/cm^3), and density will have significant influences on the volumetric heat capacity and thermal conductivity. The c for CNT-sheet (~0.6 to 0.7 J/(gK)) is higher than copper (~0.4 J/(gK)) as seen in Figure 3, but still the difference in density is of a larger magnitude and results in a larger volumetric heat capacity for copper. CNT-sheet will thus perform superiorly to copper in thermal conduction applications that require quick cooling and heating as the volumetric heat capacity is low: 0.24 J/(cm^3 K) for CNT-sheet compared to 3.4 J/(cm^3 K) for copper. Conversely, the low volumetric heat capacity reduces the thermal conductivity.

3.4. Thermal Conductivity. The in-plane calculated thermal conductivity using (1) is 25 ± 1.2 W/mK for CNT-sheet, which is considerably lower than the thermal conductivity of copper 380 W/mK. However, when considering the in-plane specific thermal conductivity, CNT-sheet (64 $W/mK/g/cm^3$) performs better than copper (43 $W/mK/g/cm^3$) due to the significantly lower density of CNT-sheets. Therefore, it can be said that CNT-sheet is more thermally conductive by weight, but lower than copper by volume.

The out-of-plane thermal conductivity of CNT-sheet was measured to be 0.10 ± 0.01 W/(mK). This value is close to that of very insulating material; thus, CNT-sheet is a good thermal insulator in the out-of-plane direction, but a good thermal conductor in the in-plane direction. Figure 4 shows a schematic of the in-plane and out-of-plane thermal conductivity of CNT-sheet. Table 1 provides an overview of the CNT-sheet and copper thermal properties.

3.5. Thermal Emittance. Heat loss can occur by thermal conduction, convection, and thermal emittance. Thermal conduction behavior has been discussed above. Convection is not a bulk material property, hence not applicable to the present thermal transport behavior of CNT-sheet. By heating a specimen in a vacuum, no convection can occur; thus, the tests were conducted under a vacuum of 10^{-5} Torr. The specimen was heated with a peltier stage. Thermal emittance is significant for high emissivity materials. The CNT-sheet tested was found to have an emissivity of 0.47 at a wavelength of 10 μm, which is the average wavelength the IR camera reads. The resulting gradients can be found in Figure 5, which validate the one-dimensional assumption, that is, (3). Figure 6 shows the temperature profile. Polynomial relations were fitted to both copper (7) and CNT-sheet (8). Both polynomial equations were a good fit with R^2 greater than 0.996. These equations were then used to find the thermal emittance properties and heat flux. A noticeable feature is that the CNT-sheet temperature gradient approaches ambient temperature within 25 mm and holds that ambient temperature further from the heater. This indicates most of the heat has been emitted in the first 25 mm and demonstrating the effectiveness of the CNT at dissipating heat. However, this change in state requires increasing the polynomial from y^4 to y^6 to

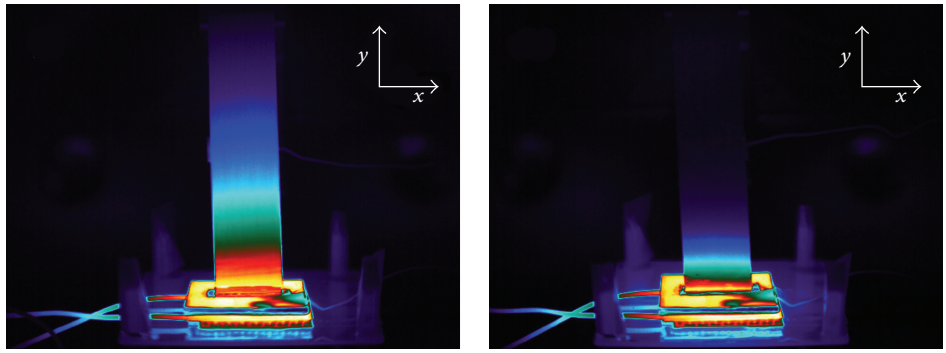

(a) (b)

Figure 5: Raw IR data of (a) copper and (b) CNT-sheet in a vacuum validating one-dimensional thermal assumption.

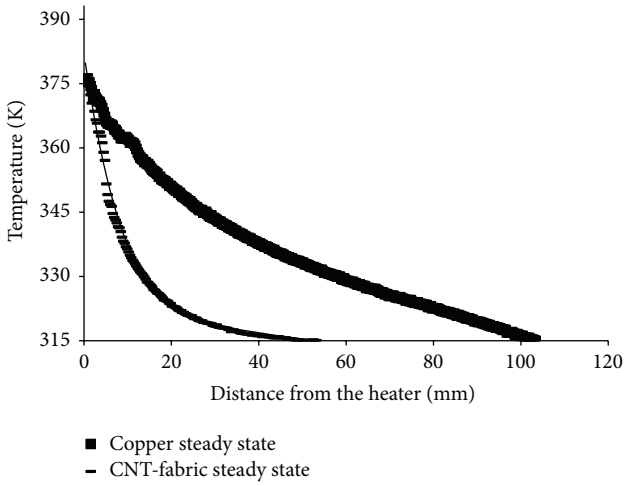

Figure 6: Temperature versus distance from the heater showing CNT-sheet cooled down considerably faster.

fit the change in state; that is, temperature is cooling down to holding at ambient temperature. The copper equation is also presented with the same number of polynomials for appropriate comparison. To verify the accuracy of the data, (3) was utilized to verify the empirical data as it follows thermal transport theory:

$$\begin{aligned}\text{Temp}_{\text{Cu}} = {} & 1.08E^{-10}y^6 - 4.49E^{-8}y^5 + 7.56E^{-6}y^4 \\ & - 7.02E^{-4}y^3 + 4.18E^{-2}y^2 - 1.94y \\ & + 1.04E^2,\end{aligned} \tag{7}$$

$$\begin{aligned}\text{Temp}_{\text{CNT}} = {} & 1.73E^{-9}y^6 - 6.69E^{-7}y^5 + 1.03E^{-4}y^4 \\ & - 7.99E^{-3}y^3 + 3.34E^{-1}y^2 - 7.31y \\ & + 1.10E^2.\end{aligned} \tag{8}$$

Figure 7 shows the calculated thermal emittance rate emitting from the CNT-sheet and copper specimens. The dashed lines in Figure 7 correspond to $R_{\text{Equation (3)}}$ and the solid line corresponds to $C_{\text{Equation (3)}}$. It is clear that these two equations' trend is as (3) would suggest, therefore indicating that (3) is capturing the relevant physics regarding the balance between conduction and thermal emittance. A more critical examination is shown in Figure 8 by normalizing the $R_{\text{Equation (3)}}$ to $C_{\text{Equation (3)}}$. This shows the normalized error and starts out near 0. The normalized error increases to maximum of 14% at 11 mm and then trends downward to 0 at 25 mm. After 25 mm, the error stays close to 0, never exceeding 8%.

A noticeable feature is that the CNT-sheet has a considerably larger thermal emittance rate than that of the copper sample, even with one side of the copper sample painted with flat black paint. Looking at the right side of (3), density in the denominator is the major difference between the CNT-sheet and copper other than emissivity. Thus, density and emissivity play important roles in rate of thermal emittance.

Copper has a significantly larger thermal conductivity (380 W/mK) compared to the tested CNT-sheet of (25 W/mK); however CNT-sheet still benefits from a larger thermal emittance which could allow for more thermal flux or cooling occurring. Looking at Figure 9, there is still a larger amount of heat flux being transferred through the copper compared to the CNT-sheet. CNT-sheet can transfer only 25% of the thermal energy that copper can transfer when conduction and thermal emittance is considered. The CNT-sheet is considerably lighter, only 4% the weight of copper. When contrasting the specific heat flux between these two materials, it can be seen that CNT-sheet has better properties compared to copper, and it is significant, that is, a 614% improvement over the "gold standard", copper. Copper's ability to transfer heat is better by volume, while CNT-sheet is superior by weight. In applications where weight is a primary concern, CNT-sheet will be able to replace heavy copper for thermal management applications leading to reduced weight. This could significantly affect the automotive, aircraft, and space industries.

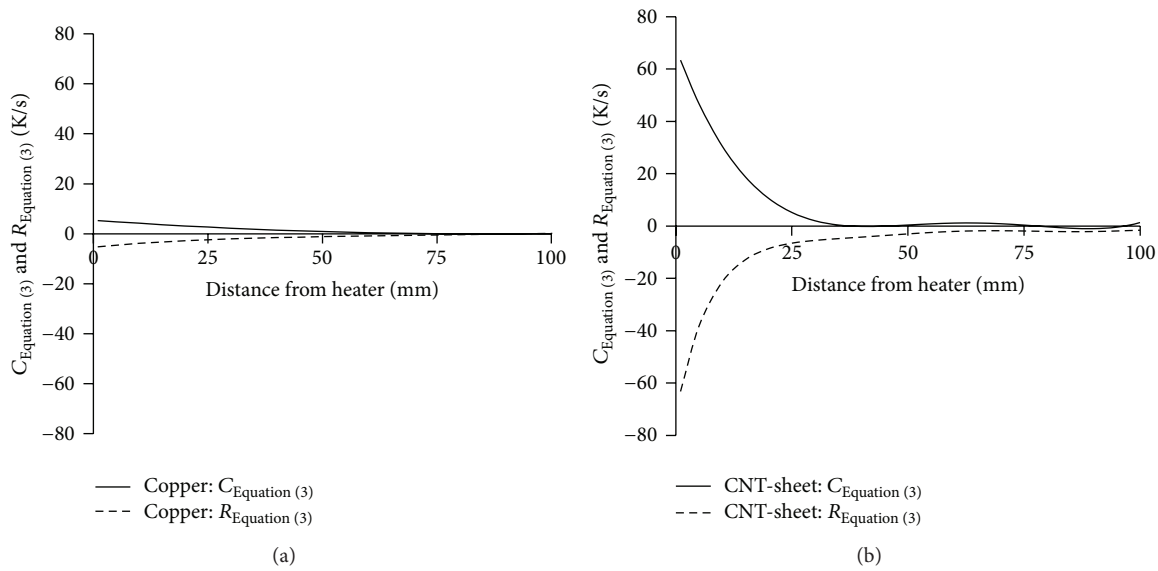

Figure 7: Thermal emittance versus distance from heater for (a) copper and (b) CNT-sheet quantifying CNT-sheet radiates more heat than copper.

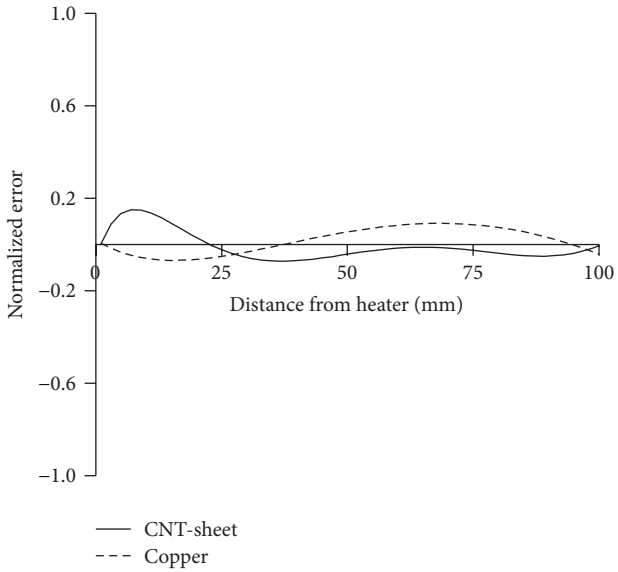

Figure 8: Normalized error of $R_{\text{Equation (3)}}$ compared to $C_{\text{Equation (3)}}$ confining error between equations.

4. Conclusion

The thermal transport properties of the dry spun low density (0.38 g/cm^3) CNT-sheet were characterized and compared with those of the copper sheet. This includes the thermal diffusivity, density, and specific heat. The thermal diffusivity of copper and CNT-sheet at room temperature is comparable within 94% of each other. The density of CNT-sheet is only 4% of copper and plays a major role in thermal conductivity and thermal emittance properties. The specific heat of CNT-sheet is larger than that of copper by 159%. These three properties lead to a calculated in-plane thermal conductivity of 25 W/mK. CNT-sheet has anisotropic properties along the in-plane and out-of-plane directions. The out-of-plane thermal conductivity was measured which was equal to 0.1 W/mK. Therefore, CNT-sheet behaves as both a thermally insulating material and a thermally conductive material depending on the orientation. This multifunctionality feature can be utilized in several applications. Furthermore, the tested CNT-sheet is a surprisingly good radiator of heat due to its low density despite of its low emissivity (0.47). CNT-sheet's ability to transfer heat flux per density is superior to that of copper, that is, by 614%. Applications that require thermal management and are sensitive to weight are ideal usage of CNT-sheet. The automobile, aircraft, and space industries, where weight amounts to high legacy costs such as fuel

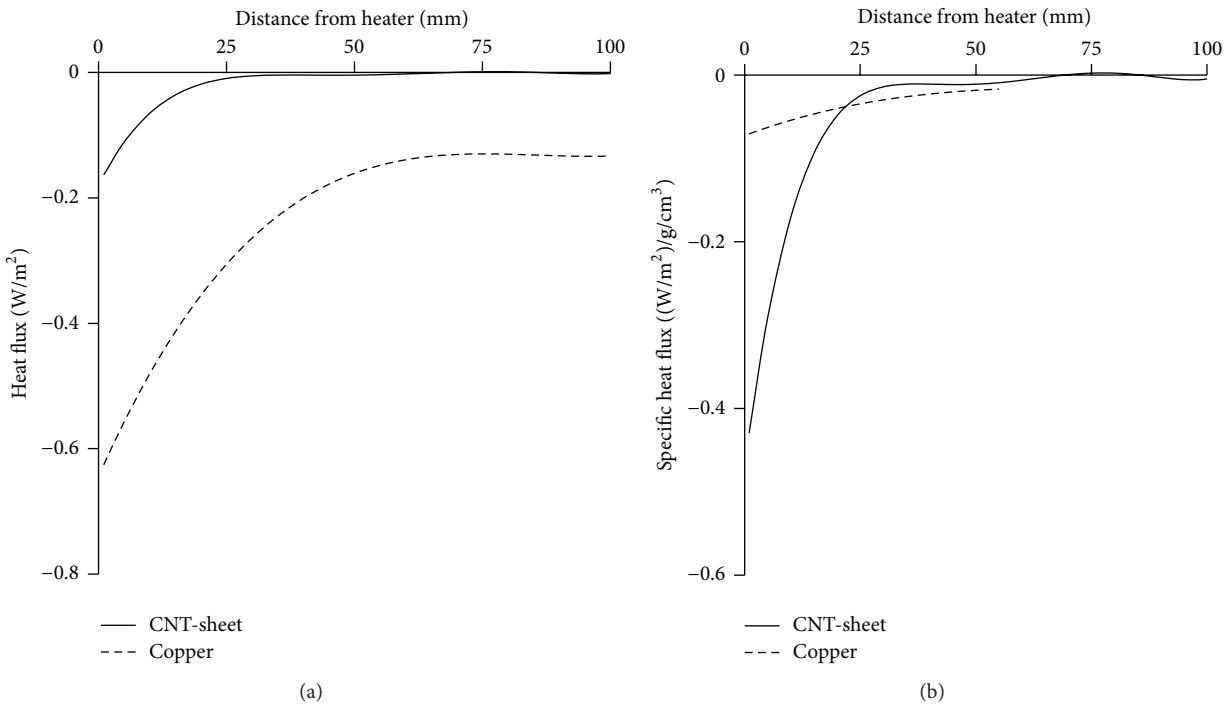

Figure 9: Quantified (a) heat flux and (b) specific heat flux versus distance from heater showing copper has better properties by volume, but CNT-sheet outperforms copper by weight.

costs, are industries where use of CNT-sheets for thermal management will make the largest impact.

Disclaimer

The views expressed in this paper are those of the authors and do not reflect the official policy or position of the United States Air Force, Department of Defense, or the US Government.

Conflict of Interests

The authors declare that there is no conflict of interests regarding the publication of this paper.

Acknowledgments

This study was partially supported by the US Air Force Office of Scientific Research (Dr. J. Harrison, AFOSR), Washington, DC.

References

[1] R. Saito, G. Dresselhaus, and M. Dresselhaus, *Physical Properties of Carbon Nanotubes*, Imperial College Press, London, UK, 1998.

[2] W. Lu, M. Zu, J.-H. Byun, B.-S. Kim, and T.-W. Chou, "State of the art of carbon nanotube fibers: opportunities and challenges," *Advanced Materials*, vol. 24, no. 14, pp. 1805–1833, 2012.

[3] R. H. Baughman, A. A. Zakhidov, and W. A. de Heer, "Carbon nanotubes—the route toward applications," *Science*, vol. 297, no. 5582, pp. 787–792, 2002.

[4] M. Zhang, K. R. Atkinson, and R. H. Baughman, "Multifunctional carbon nanotube yarns by downsizing an ancient technology," *Science*, vol. 306, no. 5700, pp. 1358–1361, 2004.

[5] H. E. Misak and S. Mall, "Investigation into microstructure of carbon nanotube multi-yarn," *Carbon*, vol. 72, pp. 321–327, 2014.

[6] H. E. Misak, V. Sabelkin, S. Mall, R. Asmatulu, and P. E. Kladitis, "Failure analysis of carbon nanotube wires," *Carbon*, vol. 50, no. 13, pp. 4871–4879, 2012.

[7] V. Sabelkin, H. E. Misak, S. Mall, R. Asmatulu, and P. E. Kladitis, "Tensile loading behavior of carbon nanotube wires," *Carbon*, vol. 50, no. 7, pp. 2530–2538, 2012.

[8] K. Koziol, J. Vilatela, A. Moisala et al., "High-performance carbon nanotube fiber," *Science*, vol. 318, no. 5858, pp. 1892–1895, 2007.

[9] M.-F. Yu, B. S. Files, S. Arepalli, and R. S. Ruoff, "Tensile loading of ropes of single wall carbon nanotubes and their mechanical properties," *Physical Review Letters*, vol. 84, no. 24, p. 5552, 2000.

[10] H. E. Misak, V. Sabelkin, S. Mall, and P. E. Kladitis, "Thermal fatigue and hypothermal atomic oxygen exposure behavior of carbon nanotube wire," *Carbon*, vol. 57, pp. 42–49, 2013.

[11] H. E. Misak, V. Sabelkin, L. Miller, R. Asmatulu, and S. Mall, "Creep and inverse stress relaxation behaviors of carbon nanotube yarns," *Journal of Nanoscience and Nanotechnology*, vol. 13, no. 12, pp. 8331–8339, 2013.

[12] A. Allaoui, S. V. Hoa, P. Evesque, and J. Bai, "Electronic transport in carbon nanotube tangles under compression: the role of contact resistance," *Scripta Materialia*, vol. 61, no. 6, pp. 628–631, 2009.

[13] H. E. Misak and S. Mall, "Electrical conductivity, strength and microstructure of carbon nanotube multi-yarns," *Materials & Design*, vol. 75, pp. 76–84, 2015.

[14] H. Misak and S. Mall, "Time-dependent electrical properties of carbon nanotube yarns," *New Carbon Materials*, vol. 30, no. 3, pp. 207–213, 2015.

[15] H. E. Misak, R. Asmatulu, M. Omalley, E. Jurak, and S. Mall, "Functionalization of carbon nanotube yarn by acid treatment," *International Journal of Smart and Nano Materials*, vol. 5, no. 1, pp. 34–43, 2014.

[16] H. Misak, R. Asmatulu, and S. Mall, "Tensile behavior of carbon nanotube multi-yarn coated with polyester," *Journal of Composite Materials*, vol. 49, no. 14, pp. 1787–1793, 2015.

[17] A. M. Marconnet, M. A. Panzer, and K. E. Goodson, "Thermal conduction phenomena in carbon nanotubes and related nanostructured materials," *Reviews of Modern Physics*, vol. 85, no. 3, pp. 1295–1326, 2013.

[18] C. Yu, L. Shi, Z. Yao, D. Li, and A. Majumdar, "Thermal conductance and thermopower of an individual single-wall carbon nanotube," *Nano Letters*, vol. 5, no. 9, pp. 1842–1846, 2005.

[19] M. T. Pettes and L. Shi, "Thermal and structural characterizations of individual single-, double-, and multi-walled carbon nanotubes," *Advanced Functional Materials*, vol. 19, no. 24, pp. 3918–3925, 2009.

[20] T. Y. Choi, D. Poulikakos, J. Tharian, and U. Sennhauser, "Measurement of thermal conductivity of individual multiwalled carbon nanotubes by the 3-ω method," *Applied Physics Letters*, vol. 87, no. 1, Article ID 013108, 2005.

[21] S. L. Kakani, *Material Science*, New Age International (P) Limited, 2006.

[22] M. J. Biercuk, M. C. Llaguno, M. Radosavljevic, J. K. Hyun, A. T. Johnson, and J. E. Fischer, "Carbon nanotube composites for thermal management," *Applied Physics Letters*, vol. 80, no. 15, pp. 2767–2769, 2002.

[23] P. Gong, P. Buahom, M. Tran, M. Saniei, C. B. Park, and P. Pötschke, "Heat transfer in microcellular polystyrene/multi-walled carbon nanotube nanocomposite foams," *Carbon*, vol. 93, pp. 819–829, 2015.

[24] H. E. Misak, R. Asmatulu, J. Whitman, and S. Mall, "High-temperature cross-linking of carbon nanotube multi-yarn using polyvinylpyrrolidone as a binding agent," *Journal of Nanoscience and Nanotechnology*, vol. 15, no. 3, pp. 2283–2288, 2015.

[25] M. B. Jakubinek, M. B. Johnson, M. A. White et al., "Thermal and electrical conductivity of array-spun multi-walled carbon nanotube yarns," *Carbon*, vol. 50, no. 1, pp. 244–248, 2012.

[26] L. Zhang, G. Zhang, C. Liu, and S. Fan, "High-density carbon nanotube buckypapers with superior transport and mechanical properties," *Nano Letters*, vol. 12, no. 9, pp. 4848–4852, 2012.

[27] M. Li and Y. Yue, "Raman-based steady-state thermal characterization of multiwall carbon nanotube bundle and buckypaper," *Journal of Nanoscience and Nanotechnology*, vol. 15, no. 4, pp. 3004–3010, 2015.

[28] A. E. Aliev, M. H. Lima, E. M. Silverman, and R. H. Baughman, "Thermal conductivity of multi-walled carbon nanotube sheets: radiation losses and quenching of phonon modes," *Nanotechnology*, vol. 21, no. 3, Article ID 035709, 2010.

[29] X. Zhang, Q. Li, Y. Tu et al., "Strong carbon-nanotube fibers spun from long carbon-nanotube arrays," *Small*, vol. 3, no. 2, pp. 244–248, 2007.

[30] M. Gustavsson, E. Karawacki, and S. E. Gustafsson, "Thermal conductivity, thermal diffusivity, and specific heat of thin samples from transient measurements with hot disk sensors," *Review of Scientific Instruments*, vol. 65, no. 12, pp. 3856–3859, 1994.

[31] ASTM, "Standard test method for thermal diffusivity of solids by the flass method," Tech. Rep. E1461-13, ASTM International, 2001.

[32] A. B. Donaldson and R. E. Taylor, "Thermal diffusivity measurement by a radial heat flow method," *Journal of Applied Physics*, vol. 46, no. 10, pp. 4584–4589, 1975.

[33] M. Zhang, S. Fang, A. A. Zakhidov et al., "Strong, transparent, multifunctional, carbon nanotube sheets," *Science*, vol. 309, no. 5738, pp. 1215–1219, 2005.

[34] X. Zhang, K. Jiang, C. Feng et al., "Spinning and processing continuous yarns from 4-inch wafer scale super-aligned carbon nanotube arrays," *Advanced Materials*, vol. 18, no. 12, pp. 1505–1510, 2006.

[35] Y. N. Zhang, G. Z. Sun, and L. X. Zheng, "Fabrication and properties of macroscopic carbon nanotube assemblies transforming from aligned nanotubes," *Journal of Nanomaterials*, vol. 2015, Article ID 907954, 8 pages, 2015.